THE JOURNAL OF PHYSICAL CHEMISTRY Letters

Letter

pubs.acs.org/JPCL

# First-Principles Study of Phosphorene and Graphene Heterostructure as Anode Materials for Rechargeable Li Batteries

Gen-Cai Guo,[†,‡] Da Wang,[‡] Xiao-Lin Wei,[*,†] Qi Zhang,[†] Hao Liu,[§,‡] Woon-Ming Lau,[‡,§] and Li-Min Liu[*,‡]

[†]Hunan Key Laboratory for Micro-Nano Energy Materials and Device, Department of Physics, Xiangtan University, Xiangtan, Hunan 411105, China

[‡]Beijing Computational Science Research Center, Beijing 100193, China

[§]Chengdu Green Energy and Green Manufacturing Technology R&D Center, Chengdu, Sichuan 610207, China

**ABSTRACT:** There is a great desire to develop the high-efficient anodes materials for Li batteries, which require not only large capacity but also high stability and mobility. In this work, the phosphorene/graphene heterostructure (P/G) was carefully explored based on first-principles calculations. The binding energy of Li on the pristine phosphorene is relatively weak (within 1.9 eV), whereas the phosphorene/graphene heterostructure (P/G) can greatly improve the binding energy (2.6 eV) without affecting the high mobility of Li within the layers. The electronic structures show that the large Li adsorption energy and fast diffusion ability of the P/G origin from the interfacial synergy effect. Interestingly, the P/G also displays ultrahigh stiffness ($C_{ac}$ = 350 N/m, $C_{zz}$ = 464 N/m), which can effectively avoid the distortion of the pristine phosphorene after the insertion of lithium. Thus, P/G can greatly enhance the cycle life of the battery. Owing to the high capacity, good conductivity, excellent Li mobility, and ultrahigh stiffness, P/G is a very promising anode material in Li-ion batteries (LIBs).

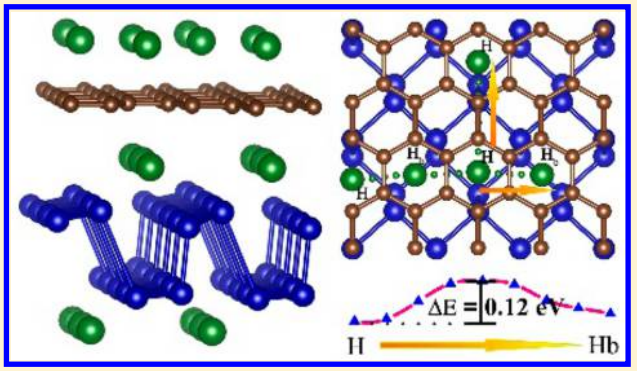


The rapid development of the electronic market reveals a breakthrough in terms of electrode materials in recent years. As one of the promising battery systems, lithium-ion batteries (LIBs) have attracted tremendous attention due to the high reversible capacity,[1,2] high energy density,[3,4] and good cycle life.[5] Moreover, LIBs are widely used as portable power sources in the diverse electronic devices such as cellular phones, notebook computers, camcorders, and wearable devices.[6,7] Many researches have been made over the past decade to increase the gravimetric and volumetric energy density of lithium ion batteries. Nowadays, graphite is used as anode material for Li-ion batteries extensively, due to its high energy stability, cycling stability, and low cost.[8,9] However, the relatively low capacity (372 mAh $g^{-1}$) and weak Li adsorption strength, which may lead to the formation of metallic lithium during the cycling of graphite restrict its further applications. The single-layered structure of graphite, called graphene, became experimentally accessible in 2004, has exhibited superior electrochemical properties in LIBs, such as the large surface areas, low migration barrier and broad voltage windows.[10,11] To date, graphene has been utilized as electrode materials and obtained great success.[2,12,13] Meanwhile, other graphene-like 2D materials such as transition metal dichalcogenides (TMD) and MXenes (M = Ti, V, Cr, Nb, etc. X = C, N) have also been widely studied and exhibit a high specific capacity and superior rate capability.[14−16] However, it is still a challenge to obtain a satisfactory electrode with the good electrical conductivity, excellent cycling stability, and rate capability.

Recently, phosphorus (P), an element of the fifth group in the periodic table, was found to be electrochemically active and could be used as a Li-ion battery anode.[17] Black phosphorus is the most stable phosphorus allotrope at room temperature.[18] The single-layered black phosphorus, named phosphorene, has been widely studied due to the graphite-like layered structure, and each phosphorus atom is covalently bonded with three adjacent phosphorus atoms to form a puckered honeycomb structure.[19,20] The high theoretical specific capacity of 2596 mAh $g^{-1}$ could be attained in the case of the uptake of lithium to form $Li_3P$.[21,22] However, the large volume change (about 300%) is observed during the lithiation process, which always results in rapid capacity fading.[17] Zhang et al.[23] employed first-principles calculations to investigate the adsorption and diffusion of Li in phosphorene, and their studies reveal that the ultrafast and directional diffusion of Li in phosphorene, which indicates the excellent fast charge/discharge capacity. Notably, the phosphorene nanoribbons and single vacancy

**Received:** November 10, 2015
**Accepted:** December 1, 2015

  

DOI: 10.1021/acs.jpclett.5b02513
J. Phys. Chem. Lett. 2015, 6, 5002−5008

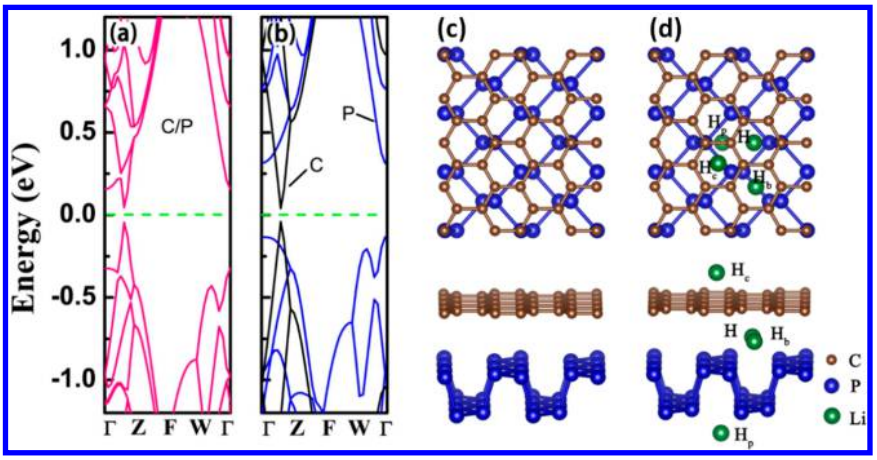


**Figure 1.** Band structures of (a) P/G (b) SG (black line) and SP (blue line). Top and side views of (c) P/G and (d) Li adsorption sites in P/G (Li/P/G, P/Li/G, and P/G/Li).

defect phosphorene can also affect the fast charge/discharge capacity.[24,25]

Despite their extensive investigations, phosphorene-based electrode materials with good electrical conductivity, high specific capacity, and excellent cyclic stability are still under development. In recent years, nanotechnology has made progress in designing novel materials. The heterostructure between the layered structures is an effective way to construct devices that integrates the properties of their isolated components. Furthermore, in order to improve the electrochemical properties and structural stability of nanoscale electrode materials, the carbon materials—such as graphene, carbon nanotube, and mesoporous carbon—are widely introduced to construct hybrid electrodes.[26−30] The phosphorus−carbon nanocomposite anodes for lithium-ion have been studied by experimental workers, which displays high initial capacities (1700 mAh $g^{-1}$).[31] Graphene composites with polymers, metals, and metal oxides have also shown good performance in LIBs due to their excellent electrical conductivity and mechanical properties.[32−34] The high specific surface area and flexibility of graphene enable good interfacial contact with particles, which can effectively prevent particle aggregation during volume contraction/expansion.[35−37] Furthermore, the hybrid phosphorus−graphene nanosheet exhibits the exceptional high-temperature cycling stability as the lithium-ion anode.[38] However, the electrochemical mechanism of phosphorene/graphene heterostructure (P/G) is not clear so far.

In our study, we have systematically investigated the Li adsorption and diffusion properties on the P/G by means of density functional theory (DFT) calculations. The energetic stability of the P/G, as well as the Li adsorption properties were first examined. The results suggest that the P/G can greatly improve the stiffness, conductivity, and the bonding strength of Li compared to the pristine single-layered phosphorus (SP). Moreover, the P/G displays the high lithium intercalation capacity without sacrificing the high mobility of Li in P/G. Our studies suggest that the P/G has great potential to be used as anode material for LIBs. We expect that our results will stimulate further developments of phosphorus-based anode materials for lithium-ion batteries.

*Results and Discussion*. As mentioned in the introduction, the material should exhibit the high capacity, mobility, and cycling properties. In order to meet the requirement of a high-efficient anode. Here, we propose the P/G heterostructure as the potential material for Li anode, and the related electronic properties, adsorption energy, diffusion, and stability are fully explored. Initially, we performed a full geometry optimization for the P/G, as shown in Figure 1c. The stacking stability ($E_f$) of P/G is examined by calculating the formation energy, which is defined in eq 1. The calculated formation energy of the P/G is 0.141 eV/atom; thus, the formation of P/G system is an exothermic process, indicating that the P/G can be used as the electrode material in LIBs. The equilibrium interlayer distance is 3.612 Å, which is comparable with the recent theoretical calculations on the 2D graphene based nanocomposites, such as G/S, G/g-BN G/g-$C_3N_4$, G/g-ZnO, and G/$MoS_2$.[49−51]

Li Adsorption on the P/G. Next, we further investigate the Li adsorption properties in the P/G. There are three typical adsorption places: (1) Li adsorption on the outside surface of phosphorene (Li/P/G), (2) Li adsorption on the outside surface of graphene (P/G/Li), and (3) Li embedded in the interlayer of P/G (P/Li/G). We performed a full geometry optimization for the structure of Li incorporation into P/G by considering a set of different adsorption sites of Li adatom. The calculated results of stable adsorption sites of Li and corresponding binding energies are shown in Figure 1d and Table 1. Some characteristics were found. First, the most stable adsorption sites of Li adsorption on both Li/P/G and P/G/Li system are similar to pristine monolayer (Li/P and Li/G) that Li adsorption above the center of the triangle that consisting of three P atoms ($H_p$ site) and that Li adsorption on the center of a hexagon of C atoms ($H_c$ site).

**Table 1. Binding Energy, $E_b$ in eV, of Absorbed One Li, Equilibrium Interlayer Distances, $d$ in Å, between Graphene and Phosphorene, and the Charge Transfer of Li, Carbon, and Phosphorus Atoms, $\Delta Q_{Li}$, $\Delta Q_C$, and $\Delta Q_P$, Respectively**

| | Li site | $E_b$(eV) | $\Delta Q_{Li}$ | $\Delta Q_C$ | $\Delta Q_P$ | $d_{C-P}$ |
|---|---|---|---|---|---|---|
| P/Li | H | 1.990 | +0.865 | | −0.865 | |
| G/Li | H | 1.301 | +0.879 | −0.879 | | |
| Li/P/G | $H_p$ | 2.125 | +0.857 | −0.204 | −0.653 | 3.568 |
| P/G/Li | $H_g$ | 1.479 | +0.877 | −0.626 | −0.251 | 3.603 |
| P/Li/G | H | 2.585 | +0.855 | −0.405 | −0.450 | 3.751 |
| | $H_b$ | 2.561 | +0.853 | −0.403 | −0.449 | 3.698 |



DOI: 10.1021/acs.jpclett.5b02513
J. Phys. Chem. Lett. 2015, 6, 5002−5008

Second, the P/Li/G system exhibits a remarkable feature that the Li atoms feel the presence of the graphene (phosphorene) sheet. Both Li binding energy and equilibrium geometry greatly depend on the atomic structure around the Li atom at the P/G interface. The Li adatom embedded in the interlayer of P/G prefers to stay at the positon of 2-fold stable site (H site) with a binding energy of 2.59 eV, which is the most stable site on both phosphorene and graphene monolayer. Meanwhile, there is a metastable adsorption site ($H_b$ site) (Figure 1d) with a slightly small binding energy (2.56 eV) compared to H site. These results suggest that the energetic stability of the Li atom in the interlayer of P/G is ruled by the phosphorene and graphene collectively. Finally, it can be seen that the P/Li/G system is energetically more stable than Li/P/G (P/G/Li) system and pristine single-layered Li/P (Li/G) system by 0.46 eV (1.11 eV) and 0.60 eV (1.28 eV), respectively. These findings indicate that Li atoms are more likely to insert into the interlayer of P/G rather than adsorption on the outside surface of phosphorene (graphene) in P/G system during the lithiation process. That is to say, Li will occupy the interlayer of the P/G first, and then take the outside surfaces of phosphorene and graphene in P/G. Besides, it can be inferred from the binding energy that the P/G heterostructure can significantly enhance the Li bonding strength compared to pristine SG or SP systems, which can be attributed by the synergistic effect. The moderate strong binding between Li and P/G can avoid the formation of metallic lithium and thus improve the safety and reversibility of Lithium-ion batteries, which is also observed in the experiment.[52] Furthermore, considering the extraction of Li atoms from these high Li binding strength P/G, we note that once $Li^+$ diffused to the edge of the electrode, and the extract energy of $Li^+$ from P/G would be strongly dependent on the cooperation of $Li^+$ with the electrolyte, which should be much lower than the $Li^+$ adsorption energy.

As the Li is further inserted into the P/G, the binding energy decreases gradually. The reduction in binding energy should come from two main factors. One is the weak electrostatic attraction between P/G host and Li cations, and the other is the enhanced Li−Li repulsion at relatively high Li concentrations. When the number of Li reaches to 20 (see the inset in Figure 6), nondistortion structure occurs, and the calculated Li binding energy is 1.66 eV, corresponding to an electrode potential of 0.06 V. The calculated electrode potential of P/G is in the range of 1.01−0.06 V during the lithiation, which is obviously higher than that in pristine phosphorene (0.39−0.12 V) in our previous work. As a result, the P/G is able to provide a much higher capacity of 485.31 mAh $g^{-1}$, which cannot be achieved by phosphorene (432.79 mAh $g^{-1}$, $Li_{0.5}P$) anode material.

Diffusion Properties. Since the Li-ion mobility is vital for the rate at which a battery may rapidly charge/discharge and hence deliver power, we next turn our attention to the mobility of Li atoms at P/G. As shown in Figure 2 and Figure 3, there are two cases of Li diffusion on the P/G: (1) Li atom diffusion on the outside surface of the P/G, and (2) Li atom diffusion in the interlayer of the P/G.

We first studied the possible diffusion paths and the energy barrier of Li on the outside surface of phosphorene and graphene (Li/P/G and P/G/Li) in P/G. As Li atoms diffuse on the outside surface of phosphorene, the most stable adsorption site for Li is $H_p$ sites. Though Li moves between two adjacent $H_p$ sites, the diffusion path is inside the groove of phosphorene (Figure 2), and the corresponding energy barrier is 0.09 eV.

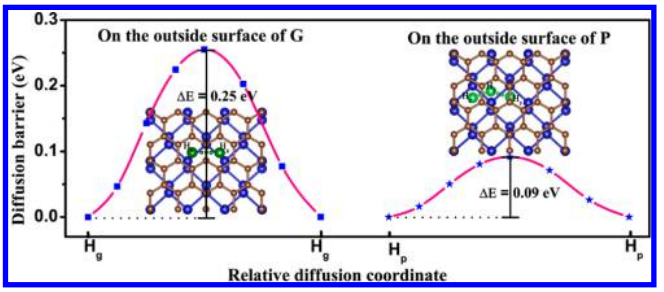


**Figure 2.** Energy barrier and diffusion path of one Li atom diffusion along the outside surface of graphene (P/G/Li) and phosphorene (Li/P/G).

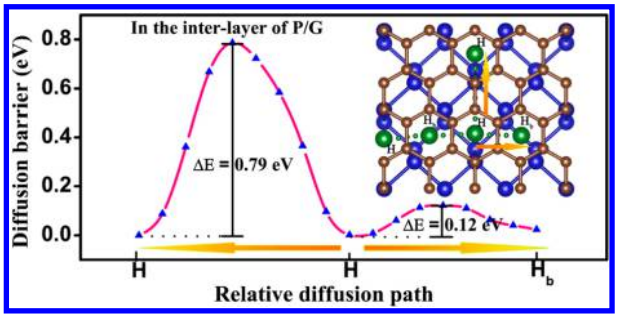


**Figure 3.** Energy barrier and diffusion path of one Li atom diffusion in the interlayer of P/G (P/Li/G). Both Li atom diffusions inside the groove of phosphorene (H−H) and between two adjacent grooves of phosphorene (H−$H_b$) are considered.

These results are fully consistent with the case of Li diffusion on the pristine SP that we have calculated before (0.09 eV).[27] As Li diffuses on the outside surface of graphene, the Li moves between two adjacent $H_g$ sites by across a C−C bridge (Figure 2), which is similar to the pristine SG. The diffusion barrier of Li move on the outside surface of graphene is 0.25 eV, which is slightly lower than the pristine SG (0.31 eV). The relatively small diffusion barrier of Li diffusion on the graphene is mainly due to the presence of phosphorene.

Next, we investigate how the Li atom diffuses in the interlayer of the P/G. There are two possible adsorption stable sites (H and $H_b$), when Li atom is embedded in the interlayer of P/G. As shown in Figure 3, the diffusion path of Li atom in the interlayer is quite similar to the pristine SP, which is inside the groove. The diffusion between two H sites across one $H_b$ site as an intermediate state. Notably, the diffusion of Li in the interlayer of the P/G with an energy barrier of 0.12 eV, which is slightly large (0.03 eV) compared to the pristine SP (0.09 eV). Besides, we also calculated the energy barrier of Li diffusing between two H sites directly across the groove of phosphorene, and the result indicate that this process is impossible because of the high energy barrier (0.79 eV).

Overall, the above-mentioned results imply that the energy barrier of Li diffuse on the outside surface of graphene is decreased compared to pristine SG. Meanwhile, there is no significant increase of energy barrier when Li diffuse on the outside surface of phosphorene and in the interlayer of P/G compared to pristine SP. That is to say, the pristine SP fast charge/discharge capability is still preserved in P/G. These excellent performance indicating that there is great potential for P/G as anode material for the application of LIBs.

Electronic Properties. To obtain a further understanding of the interaction between Li and P/G, we investigate the partial



DOI: 10.1021/acs.jpclett.5b02513
J. Phys. Chem. Lett. 2015, 6, 5002−5008

density of state of P/G, P/Li/G, P/G/Li and Li/P/G system, as shown in Figure 4. For P/G, the state near the Fermi level is

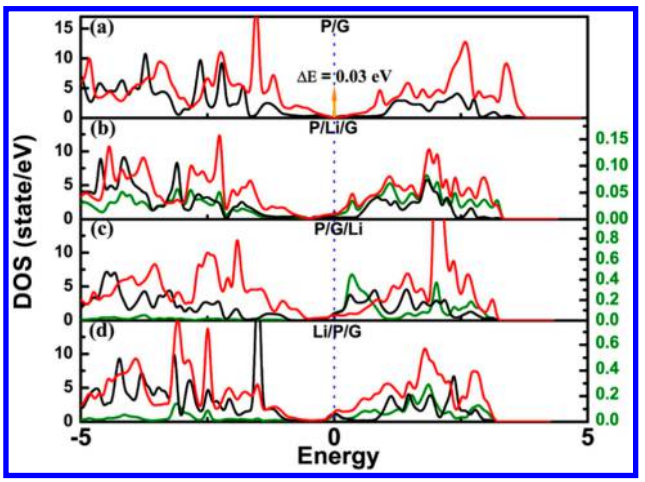


**Figure 4.** Density of state of P/G, P/Li/G, P/G/Li, and Li/P/G; black, red, and green lines represent the PDOS of C, P, and Li, respectively. The left axis is the PDOS of P and G; the right axis is the PDOS of Li.

nearly flat and with a small bandgap of 0.03 eV, as discussed in the previous research.[53] The small bandgap could be seen more clearly from the band structure in Figure 1. This is different with the pristine SP (with a band gap of 0.95 eV) and graphene (without a band gap). As can be seen, the electronic structure of P/G mimics both the phosphorene and the graphene.

After Li incorporation into P/G, the P/Li/G, P/G/Li, and Li/P/G systems become metallic (Figure 4), indicating the electron transfer from Li atoms to P/G. This phenomenon is also found in $MoS_2$/Graphene heterostructure, which is converted from semiconducting to metallic after lithiation.[54] As the Li atom adsorption on the outside surface of phosphorene (Li/P/G) and graphene (P/G/Li), the orbitals of Li overlap with phosphorene and graphene, respectively, which is the feature of covalent hybridization interactions (Figure 4c,d). These feature is also found in the pristine SP and SG. On the other hand, as Li atom embedded into the interlayer of the P/G (P/Li/G), as shown in Figure 4b, the orbitals of both phosphorene and graphene overlap with Li, indicating the covalent hybridization interactions of embedded Li with phosphorene and graphene. Furthermore, the relative small band gap of P/G is of great benefit for the electrode conductivity, which is also suggested by the experiment.[55]

To clarify the ion bond strength, we quantitatively estimate the amount of charge transfer between the adsorbed Li and P/G through Bader charge analysis for all the compositions. The results are listed in Table 1. As Li atom adsorption on the outside surface of P/G, two cases were considered. First, when one Li atom adsorption on the outside surface of phosphorene (Li/P/G), the corresponding charge of Li is +0.857 |e|, while the calculated charges of phosphorene and graphene are −0.653 |e| and −0.204 |e|, respectively ($H_p$ site). This result reveals that the charge of Li atom is transferred to the adjacent P atoms, and the interaction between the adsorbed Li atom and P atoms are predominantly ionic. Moreover, when one Li atom adsorption on the outside surface of graphene (P/G/Li), the calculated charges of phosphorene and graphene are −0.251 |e|

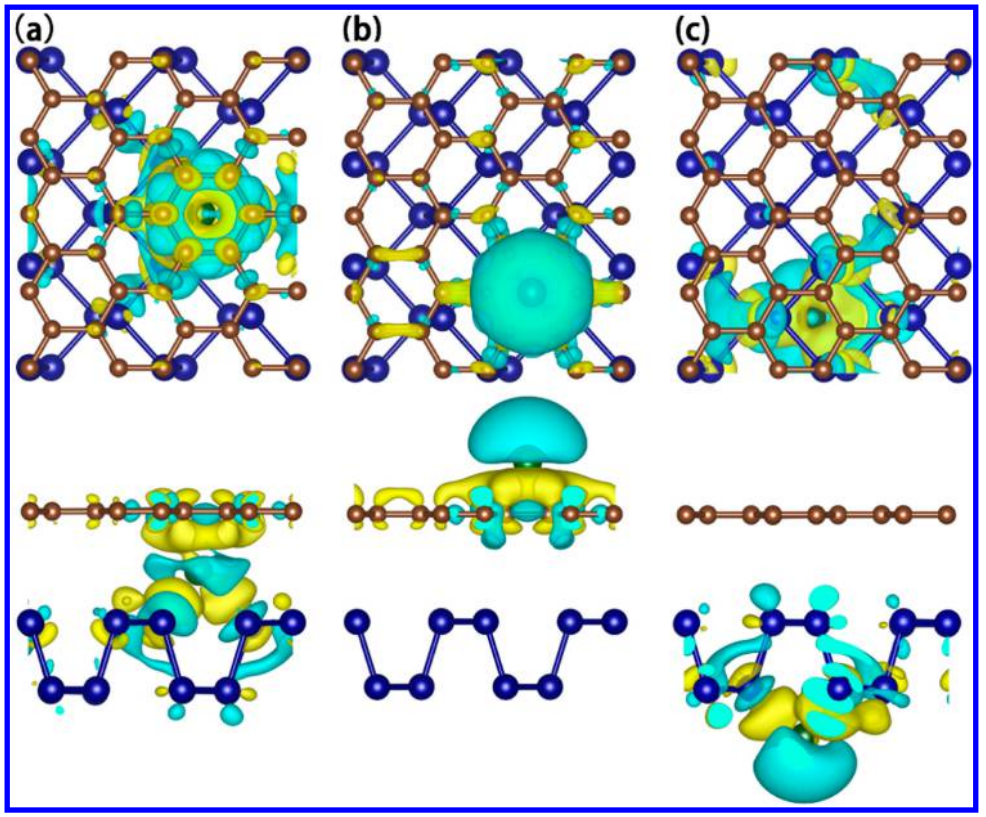


**Figure 5.** Top and side view of the diff charge density of one Li (a) insert into interlayer of G/P; (b) adsorption on the out-surface of graphene; (c) adsorption on the out-surface of phosphorene. The loss of electrons is indicated in blue and gain of electrons is indicated in yellow.



DOI: 10.1021/acs.jpclett.5b02513
J. Phys. Chem. Lett. 2015, 6, 5002−5008

and −0.626 |e|, respectively ($H_g$ site). Similar with Li/P/G system, the charge of adsorbed Li is transferred to adjacent C atoms, and the interaction between the adsorbed Li atom and C atoms are predominantly ionic.

Besides, as one Li atom is embedded in the interlayer of the P/G (H site), the charge of Li transfer to phosphorene and graphene with 0.450 |e| and 0.405 |e|, respectively. It can be seen that the obtained charge from Li to phosphorene and graphene is quite close. The phosphorene gained slightly more charge compared to graphene, which is mainly due to the stronger electronegative difference between P and Li atom. Besides, more transferred charge of absorbed Li on the H site than the $H_b$ site also confirmed that the H site is more stable than $H_b$ site. Above all, all the Li incorporation configurations show obvious charge transfer from Li to P/G, which strongly supports the strong ionic interaction between Li and P/G.

To visualize the ion bond of Li incorporation at the different sites, we calculated the charge density difference with the following equation:[56]

$$\Delta\rho(\mathrm{r}) = \rho_{\mathrm{P/G+Li}}(r) - \rho_{\mathrm{P/G}}(r) - \rho_{\mathrm{Li}}(r)$$

where $\rho_{\mathrm{P/G+Li}}(r)$ represents the charge density of Li incorporation into P/G, $\rho_{\mathrm{P/G}}(r)$ is the charge density of the P/G, and $\rho_{\mathrm{Li}}(r)$ is the charge density of isolated Li atoms in the same position as in the total systems. Figure 5a−c shows the charge density difference of Li atoms incorporation into P/G systems (P/Li/G, P/G/Li, and Li/P/G).

For the case of Li atom embedded in the interlayer of P/G (Figure 5a), a net loss of electronic charge could be found above the Li and also a net gain of electronic charge was found on its adjacent P and C atoms. The large gains in charge demonstrate the significant electronic transfer from Li atom to the neighboring P and C atoms, which indicates the strong ionic bonding of the embedded Li atom. Besides, as the Li atom adsorption on the outside surface of phosphorene and graphene, which is shown in Figure 5b−c. Most of the charge of Li is transferred to the adjacent P atom (Li/P/G system) or C atoms (P/G/Li system). These findings are consistent with the previous Bader analysis, which further verify the strong ionic interaction between Li and P/G.

Mechanical Properties. It is known that the large changes might arise in the mechanical properties of electrode materials during lithiation process, especially alloys. Additionally, the deformations due to Li insertion can cause the electrode fracture or change its morphology, eventually leading to large capacity fading and poor cycle capacities. In order to examine the stability of P/G during the lithiation, we calculated the stiffness of P/G.

The stiffness $C_{2D}$ is defined as $C_{2D} = 2(E - E_0)/[A_0(\Delta L_i/L_i)^2]$, where $E$ and $E_0$ are the total energy with lattice changes in the $i$ direction and at an equilibrium state, respectively, the $A_0$ is the area of the 2D material at the equilibrium state, $\Delta L_i$ and $L_i$ are the changes of lattice constant by strain and the pristine lattice constant of the 2D material in the $i$ direction, respectively. In this study, the lattice compression or dilatation of 2D material is about 3% ($\Delta L_i/L_i$) in the $i$ direction.

The calculated in-plane stiffness for pristine SP is calculated to be $C_{ac}$ = 31 N/m (armchair) and $C_{zz}$ = 103 N/m (zigzag), respectively, as shown in Figure 6. Interestingly, the in-plane stiffness of phosphorene in the zigzag direction is about three times larger than in the armchair direction, indicating the anisotropic nature of the material, which is in good agreement with the previous studies.[57] Besides, the stiffness of graphene in armchair and zigzag direction is almost constant. As for the P/G, the stiffness of SP for either armchair or zigzag direction is greatly enhanced compared to that of the pristine SP. Such result indicates the SP within the P/G can withstand large strains without breaking compared with the pristine SP. This high stiffness of P/G is rather vital as its application in Li-ion batteries due to the large stresses and deformations caused by the lithium insertion. Besides, the discrepancies of the proportion of in-plane stiffness between armchair ($C_{ac}$= 350 N/m) and zigzag ($C_{zz}$ = 464 N/m) direction become small, which suggests that the phosphorene with the anisotropic stiffness could be degenerated by the combination with the isotropy stiffness of graphene. This result uncover the reason for the enhanced stability of P/G, as observed in the experiment.[52]

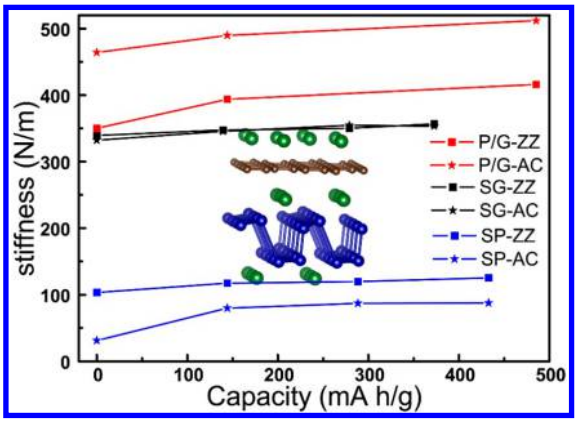


**Figure 6.** Stiffness of P/G, SG, and SP in zigzag and armchair direction with different lithium intercalation concentration. The insert is the optimized stable configuration of 20 Li atom insert into the P/G ($Li_{20}C_{32}P_{24}$).

*Conclusions*. In summary, we have systematically investigated the P/G as anode material for Li-ion batteries based on first-principles calculations. Our results indicate that the binding energy of Li incorporation into the P/G is significantly improved compared to the pristine phosphorene or graphene. Furthermore, the P/G possess ultrahigh stiffness ($C_{ac}$ = 350 N/m, $C_{zz}$ = 464 N/m) compared to pristine phosphorene ($C_{ac}$ = 31 N/m, $C_{zz}$ = 103 N/m), maintaining the high diffusion mobility of Li that on the pristine phosphorene. The calculated electronic structure reveals that the P/G owns a small band gap, indicating the enhanced conductivity compared to pristine phosphorene. Besides, the capacity of P/G system (485.31 mAh $g^{-1}$) is also greatly improved compared to the pristine phosphorene. Overall, our findings show that the P/G exhibits the extraordinary ultrahigh stiffness, high capacity, good conductivity, and excellent Li mobility; thus, the P/G should be a good candidate for the application of as an electrode material in LIBs. Moreover, these studies could enhance the understanding of 2D phosphorene-based heterostructures, which is important for the rational design of high-performance electrode materials for LIBs.

## COMPUTATIONAL METHODS

Our calculations were performed based on the density functional theory (DFT), within the general gradient approximation of Perdew−Burke−Ernzerhof (GGA-PBE) approach as implemented in the Vienna Ab-initio Simulation Package (VASP).[39,40] An energy cutoff of 500 eV was applied


DOI: 10.1021/acs.jpclett.5b02513
J. Phys. Chem. Lett. 2015, 6, 5002−5008

for the plane-wave expansion of the electronic eigenfunctions. All the structures were relaxed, including the cells, until the forces was less than $10^{-2}$ eV/Å, and the energy convergence with the energy difference is below $10^{-5}$ eV between two consecutive self-consistent steps. A vacuum of 15 Å between the layers was considered. G-point sampling was used and with 3 × 3 × 1 k points for the integration of Brillouin zone. Considering the fact that the interlayer interaction in P/G is weak van der Waals (vdW), we employed the vdW-DF scheme[41] to describe P/G systems, in order to better describe their interlayer interactions.

A new 2D graphene/phosphorene heterostructure was explored, which contains 32 carbon atoms and 24 phosphorus atoms as shown in Figure 1c. In order to minimize the lattice mismatch effects between phosphorene and graphene, we have considered a surface (or interface) periodicity of 3 × 2 and 4 × 2 for the phosphorene and graphene, respectively. To understand the Li diffusion, the diffusion barriers were explored using the climbing image nudged elastic band (CI-NEB) method.[42] Besides, the charge distribution after Li atom incorporation into P/G system was analyzed by the grid-based Bader analysis algorithm.[43] Although the lattice parameters obtained by PBE are slightly overestimated, the PBE and HSE functionals gives the similar physical trend on phophorene and graphene systems, as shown in the previous work.[44−46] Thus, all results on the electrochemical properties of P/G system are based on the PBE functional in this work.

The stacking stability ($E_f$) of P/G were calculated by the following equation

$$E_f = \frac{(E_P + E_G - E_{P/G})}{m} \quad (1)$$

where $E_f$ is the formation energy of the P/G, $E_P$ and $E_G$ are the total energies of pristine single-layered phosphorus (SP) and graphite (SG), respectively. $E_{P/G}$ is the total energy of the P/G, and $m$ is the total number of atoms in P/G. In addition, the binding energy per atom for the adsorption of $n$ Li atoms is defined by following equation:

$$E_b = \frac{(E_{P/G} + nE_{Li} - E_{P/G+Li_n})}{n} \quad (2)$$

where $E_{Li}$ is the energy of an isolated Li atom. Here, the larger value of $E_b$ represents the relatively stronger binding between Li and P/G. The average intercalation voltage, $V_{avg}$ can be determined by[47,48]

$$V_{avg} = -\frac{\Delta G}{\Delta x}$$

where $\Delta x$ refers to the number of $Li^+$ transferred, $\Delta G$ is the difference of Gibbs free energy for the intercalation reaction. Considering the small changes in volume and entropy, $\Delta G$ can be approximately calculated by the total energy difference between $Li_{x2}P/G$ and the sum of $Li_{x1}P/G$ and bulk Li.

## AUTHOR INFORMATION


### Corresponding Authors

*E-mail: limin.liu@csrc.ac.cn.
*E-mail: xlw@xtu.edu.cn.


### Notes

The authors declare no competing financial interest.

## ACKNOWLEDGMENTS

This work was supported by the National Natural Science Foundation of China (No. 51222212, 11204262, 51472209, and U1401241), the Research Foundation of Education Bureau of Hunan Province, China (Grant No. 15B237), the Young Core Instructor from the Education Bureau of Hunan Province, China (Grant No. 20151053007), and the Program for Changjiang Scholars and Innovative Research Team in University (IRT13093).

## REFERENCES


(1) Idota, Y.; Kubota, T.; Matsufuji, A.; Maekawa, Y.; Miyasaka, T. Tin-based amorphous oxide: a high-capacity lithium-ion-storage material. *Science* **1997**, *276* (5317), 1395−1397.

(2) Yoo, E.; Kim, J.; Hosono, E.; Zhou, H.-S.; Kudo, T.; Honma, I. Large reversible Li storage of graphene nanosheet families for use in rechargeable lithium ion batteries. *Nano Lett.* **2008**, *8* (8), 2277−2282.

(3) Tarascon, J.-M.; Armand, M. Issues and challenges facing rechargeable lithium batteries. *Nature* **2001**, *414* (6861), 359−367.

(4) Oyama, N.; Tatsuma, T.; Sato, T.; Sotomura, T. Dimercaptan−polyaniline composite electrodes for lithium batteries with high energy density. *Nature* **1995**, *373*, 598−600.

(5) Ji, L.; Lin, Z.; Alcoutlabi, M.; Zhang, X. Recent developments in nanostructured anode materials for rechargeable lithium-ion batteries. *Energy Environ. Sci.* **2011**, *4* (8), 2682−2699.

(6) Wang, Y.; Cao, G. Developments in Nanostructured Cathode Materials for High-Performance Lithium-Ion Batteries. *Adv. Mater.* **2008**, *20* (12), 2251−2269.

(7) Derrien, G.; Hassoun, J.; Panero, S.; Scrosati, B. Nanostructured Sn−C composite as an advanced anode material in high-performance Lithium-ion batteries. *Adv. Mater.* **2007**, *19* (17), 2336−2340.

(8) Aurbach, D.; Zinigrad, E.; Cohen, Y.; Teller, H. A short review of failure mechanisms of lithium metal and lithiated graphite anodes in liquid electrolyte solutions. *Solid State Ionics* **2002**, *148* (3), 405−416.

(9) Yoshio, M.; Wang, H.; Fukuda, K. Spherical Carbon-Coated Natural Graphite as a Lithium-Ion Battery-Anode Material. *Angew. Chem.* **2003**, *115* (35), 4335−4338.

(10) Novoselov, K. S.; Geim, A. K.; Morozov, S.; Jiang, D.; Zhang, Y.; Dubonos, S.; Grigorieva, I.; Firsov, A. Electric field effect in atomically thin carbon films. *Science* **2004**, *306* (5696), 666−669.

(11) Britnell, L.; Gorbachev, R.; Jalil, R.; Belle, B.; Schedin, F.; Mishchenko, A.; Georgiou, T.; Katsnelson, M.; Eaves, L.; Morozov, S. Field-effect tunneling transistor based on vertical graphene heterostructures. *Science* **2012**, *335* (6071), 947−950.

(12) Park, M.-S.; Yu, J.-S.; Kim, K. J.; Jeong, G.; Kim, J.-H.; Jo, Y.-N.; Hwang, U.; Kang, S.; Woo, T.; Kim, Y.-J. One-step synthesis of a sulfur-impregnated graphene cathode for lithium−sulfur batteries. *Phys. Chem. Chem. Phys.* **2012**, *14* (19), 6796−6804.

(13) Wang, H.; Yang, Y.; Liang, Y.; Robinson, J. T.; Li, Y.; Jackson, A.; Cui, Y.; Dai, H. Graphene-wrapped sulfur particles as a rechargeable lithium−sulfur battery cathode material with high capacity and cycling stability. *Nano Lett.* **2011**, *11* (7), 2644−2647.

(14) Jing, Y.; Zhou, Z.; Cabrera, C. R.; Chen, Z. Metallic VS2 monolayer: a promising 2D anode material for lithium ion batteries. *J. Phys. Chem. C* **2013**, *117* (48), 25409−25413.

(15) Li, Y.; Wu, D.; Zhou, Z.; Cabrera, C. R.; Chen, Z. Enhanced li adsorption and diffusion on MoS2 zigzag nanoribbons by edge effects: a computational study. *J. Phys. Chem. Lett.* **2012**, *3* (16), 2221−2227.

(16) Tang, Q.; Zhou, Z.; Shen, P. Are MXenes Promising Anode Materials for Li Ion Batteries? Computational Studies on Electronic Properties and Li Storage Capability of Ti3C2 and Ti3C2X2 (X = F, OH) Monolayer. *J. Am. Chem. Soc.* **2012**, *134* (40), 16909−16916.

(17) Sun, J.; Zheng, G.; Lee, H.-W.; Liu, N.; Wang, H.; Yao, H.; Yang, W.; Cui, Y. Formation of Stable Phosphorus−Carbon Bond for Enhanced Performance in Black Phosphorus Nanoparticle−Graphite Composite Battery Anodes. *Nano Lett.* **2014**, *14* (8), 4573−4580.




DOI: 10.1021/acs.jpclett.5b02513
*J. Phys. Chem. Lett.* 2015, 6, 5002−5008

(18) Bridgman, P. TWO NEW MODIFICATIONS OF PHOSPHORUS. *J. Am. Chem. Soc.* **1914**, *36* (7), 1344−1363.
(19) Liu, H.; Neal, A. T.; Zhu, Z.; Luo, Z.; Xu, X.; Tománek, D.; Ye, P. D. Phosphorene: an unexplored 2D semiconductor with a high hole mobility. *ACS Nano* **2014**, *8* (4), 4033−4041.
(20) Li, L.; Yu, Y.; Ye, G. J.; Ge, Q.; Ou, X.; Wu, H.; Feng, D.; Chen, X. H.; Zhang, Y. Black phosphorus field-effect transistors. *Nat. Nanotechnol.* **2014**, *9* (5), 372−377.
(21) Stan, M. C.; von Zamory, J.; Passerini, S.; Nilges, T.; Winter, M. Puzzling out the origin of the electrochemical activity of black P as a negative electrode material for lithium-ion batteries. *J. Mater. Chem. A* **2013**, *1* (17), 5293−5300.
(22) Li, W.-J.; Chou, S.-L.; Wang, J.-Z.; Liu, H.-K.; Dou, S.-X. Simply mixed commercial red phosphorus and carbon nanotube composite with exceptionally reversible sodium-ion storage. *Nano Lett.* **2013**, *13* (11), 5480−5484.
(23) Li, W.; Yang, Y.; Zhang, G.; Zhang, Y.-W. Ultrafast and Directional Diffusion of Lithium in Phosphorene for High-Performance Lithium-Ion Battery. *Nano Lett.* **2015**, *15* (3), 1691−1697.
(24) Yao, Q.; Huang, C.; Yuan, Y.; Liu, Y.; Liu, S.; Deng, K.; Kan, E. Theoretical Prediction of Phosphorene and Nanoribbons As Fast-Charging Li Ion Battery Anode Materials. *J. Phys. Chem. C* **2015**, *119* (12), 6923−6928.
(25) Guo, G.-C.; Wei, X.-L.; Wang, D.; Luo, Y.; Liu, L.-M. Pristine and defect-containing phosphorene as promising anode materials for rechargeable Li batteries. *J. Mater. Chem. A* **2015**, *3* (21), 11246−11252.
(26) Wang, D.; Choi, D.; Li, J.; Yang, Z.; Nie, Z.; Kou, R.; Hu, D.; Wang, C.; Saraf, L. V.; Zhang, J. Self-assembled TiO2−graphene hybrid nanostructures for enhanced Li-ion insertion. *ACS Nano* **2009**, *3* (4), 907−914.
(27) Tung, V. C.; Chen, L.-M.; Allen, M. J.; Wassei, J. K.; Nelson, K.; Kaner, R. B.; Yang, Y. Low-temperature solution processing of graphene− carbon nanotube hybrid materials for high-performance transparent conductors. *Nano Lett.* **2009**, *9* (5), 1949−1955.
(28) Jiang, H.; Ma, J.; Li, C. Mesoporous carbon incorporated metal oxide nanomaterials as supercapacitor electrodes. *Adv. Mater.* **2012**, *24* (30), 4197−4202.
(29) Guo, S.; Wen, D.; Zhai, Y.; Dong, S.; Wang, E. Platinum nanoparticle ensemble-on-graphene hybrid nanosheet: one-pot, rapid synthesis, and used as new electrode material for electrochemical sensing. *ACS Nano* **2010**, *4* (7), 3959−3968.
(30) Wang, H.; Cui, L.-F.; Yang, Y.; Sanchez Casalongue, H.; Robinson, J. T.; Liang, Y.; Cui, Y.; Dai, H. Mn3O4− graphene hybrid as a high-capacity anode material for lithium ion batteries. *J. Am. Chem. Soc.* **2010**, *132* (40), 13978−13980.
(31) Ramireddy, T.; Xing, T.; Rahman, M. M.; Chen, Y.; Dutercq, Q.; Gunzelmann, D.; Glushenkov, A. M. Phosphorus−carbon nanocomposite anodes for lithium-ion and sodium-ion batteries. *J. Mater. Chem. A* **2015**, *3* (10), 5572−5584.
(32) Zhou, G.; Wang, D.-W.; Li, F.; Zhang, L.; Li, N.; Wu, Z.-S.; Wen, L.; Lu, G. Q.; Cheng, H.-M. Graphene-wrapped Fe3O4 anode material with improved reversible capacity and cyclic stability for lithium ion batteries. *Chem. Mater.* **2010**, *22* (18), 5306−5313.
(33) Song, Z.; Xu, T.; Gordin, M. L.; Jiang, Y.-B.; Bae, I.-T.; Xiao, Q.; Zhan, H.; Liu, J.; Wang, D. Polymer−graphene nanocomposites as ultrafast-charge and-discharge cathodes for rechargeable lithium batteries. *Nano Lett.* **2012**, *12* (5), 2205−2211.
(34) Huang, X.; Qi, X.; Boey, F.; Zhang, H. Graphene-based composites. *Chem. Soc. Rev.* **2012**, *41* (2), 666−686.
(35) Zhou, X.; Yin, Y.-X.; Wan, L.-J.; Guo, Y.-G. Facile synthesis of silicon nanoparticles inserted into graphene sheets as improved anode materials for lithium-ion batteries. *Chem. Commun.* **2012**, *48* (16), 2198−2200.
(36) Xin, X.; Zhou, X.; Wang, F.; Yao, X.; Xu, X.; Zhu, Y.; Liu, Z. A 3D porous architecture of Si/graphene nanocomposite as high-performance anode materials for Li-ion batteries. *J. Mater. Chem.* **2012**, *22* (16), 7724−7730.
(37) Luo, J.; Zhao, X.; Wu, J.; Jang, H. D.; Kung, H. H.; Huang, J. Crumpled graphene-encapsulated Si nanoparticles for lithium ion battery anodes. *J. Phys. Chem. Lett.* **2012**, *3* (13), 1824−1829.
(38) Yu, Z.; Song, J.; Gordin, M. L.; Yi, R.; Tang, D.; Wang, D. Phosphorus-Graphene Nanosheet Hybrids as Lithium-Ion Anode with Exceptional High-Temperature Cycling Stability. *Advanced Science* **2015**, *2*, 1−2 DOI: 10.1002/advs.201400020.
(39) Perdew, J. P.; Burke, K.; Ernzerhof, M. Generalized gradient approximation made simple. *Phys. Rev. Lett.* **1996**, *77* (18), 3865.
(40) Kresse, G.; Furthmüller, J. Efficient iterative schemes for ab initio total-energy calculations using a plane-wave basis set. *Phys. Rev. B: Condens. Matter Mater. Phys.* **1996**, *54* (16), 11169.
(41) Klimeš, J.; Bowler, D. R.; Michaelides, A. Van der Waals density functionals applied to solids. *Phys. Rev. B: Condens. Matter Mater. Phys.* **2011**, *83* (19), 195131.
(42) Henkelman, G.; Uberuaga, B. P.; Jónsson, H. A climbing image nudged elastic band method for finding saddle points and minimum energy paths. *J. Chem. Phys.* **2000**, *113* (22), 9901−9904.
(43) Sanville, E.; Kenny, S. D.; Smith, R.; Henkelman, G. Improved grid-based algorithm for Bader charge allocation. *J. Comput. Chem.* **2007**, *28* (5), 899−908.
(44) Wang, V.; Kawazoe, Y.; Geng, W. Native point defects in few-layer phosphorene. *Phys. Rev. B: Condens. Matter Mater. Phys.* **2015**, *91* (4), 045433.
(45) Li, Y.; Chen, Z. XH/$\pi$ (X= C, Si) interactions in graphene and silicene: weak in strength, strong in tuning band structures. *J. Phys. Chem. Lett.* **2013**, *4* (2), 269−275.
(46) Li, Y.; Yang, S.; Li, J. Modulation of the electronic properties of ultrathin black phosphorus by strain and electrical field. *J. Phys. Chem. C* **2014**, *118* (41), 23970−23976.
(47) Aydinol, M.; Kohan, A.; Ceder, G.; Cho, K.; Joannopoulos, J. Ab initio study of lithium intercalation in metal oxides and metal dichalcogenides. *Phys. Rev. B: Condens. Matter Mater. Phys.* **1997**, *56* (3), 1354.
(48) Courtney, I.; Tse, J.; Mao, O.; Hafner, J.; Dahn, J. Ab initio calculation of the lithium-tin voltage profile. *Phys. Rev. B: Condens. Matter Mater. Phys.* **1998**, *58* (23), 15583.
(49) Sławińska, J.; Zasada, I.; Klusek, Z. Energy gap tuning in graphene on hexagonal boron nitride bilayer system. *Phys. Rev. B: Condens. Matter Mater. Phys.* **2010**, *81* (15), 155433.
(50) Du, A.; Sanvito, S.; Li, Z.; Wang, D.; Jiao, Y.; Liao, T.; Sun, Q.; Ng, Y. H.; Zhu, Z.; Amal, R. Hybrid graphene and graphitic carbon nitride nanocomposite: gap opening, electron−hole puddle, interfacial charge transfer, and enhanced visible light response. *J. Am. Chem. Soc.* **2012**, *134* (9), 4393−4397.
(51) Ma, Y.; Dai, Y.; Guo, M.; Niu, C.; Huang, B. Graphene adhesion on MoS 2 monolayer: An ab initio study. *Nanoscale* **2011**, *3* (9), 3883−3887.
(52) Park, C. M.; Sohn, H. J. Black phosphorus and its composite for lithium rechargeable batteries. *Adv. Mater.* **2007**, *19* (18), 2465−2468.
(53) Hu, W.; Wang, T.; Yang, J. Tunable Schottky contacts in hybrid graphene−phosphorene nanocomposites. *J. Mater. Chem. C* **2015**, *3* (18), 4756−4761.
(54) Chang, K.; Chen, W. L-cysteine-assisted synthesis of layered MoS2/graphene composites with excellent electrochemical performances for lithium ion batteries. *ACS Nano* **2011**, *5* (6), 4720−4728.
(55) Sun, J.; Lee, H.-W.; Pasta, M.; Yuan, H.; Zheng, G.; Sun, Y.; Li, Y.; Cui, Y. A phosphorene−graphene hybrid material as a high-capacity anode for sodium-ion batteries. *Nat. Nanotechnol.* **2015**, *10*, 980−985.
(56) Persson, K.; Sethuraman, V. A.; Hardwick, L. J.; Hinuma, Y.; Meng, Y. S.; van der Ven, A.; Srinivasan, V.; Kostecki, R.; Ceder, G. Lithium diffusion in graphitic carbon. *J. Phys. Chem. Lett.* **2010**, *1* (8), 1176−1180.
(57) Kulish, V. V.; Malyi, O. I.; Persson, C.; Wu, P. Phosphorene as an Anode Material for Na-Ion Batteries: A First-Principles Study. *Phys. Chem. Chem. Phys.* **2015**, *17* (21), 13921−13928.


DOI: 10.1021/acs.jpclett.5b02513
*J. Phys. Chem. Lett.* 2015, 6, 5002−5008